Absorptivity of Carbon Dioxide and Molecular Oxygen at 193 nm at High Temperatures up to 1600°C

Authors: Rice S.F.; Hanush R.G.

Source: Applied Spectroscopy, 1 December 2002, vol. 56, no. 12, pp. 1621-1625(5)

Publisher: Society for Applied Spectroscopy

Abstract

The absorptivity of CO_2 and O_2 at 193 nm must be accounted for develop a quantitative ELIF method for the detection of NaOH(gas) in glass melting furnaces. In this appendix we describe measurements of CO_2 and O_2 at 193 nm absorbtivity over the temperature range of 900–1600 °C. The data were collected in a flow-type tube furnace using an ArF excimer laser at the light source. CO_2 was mixed at 5% by volume in N_2 and O_2 was examined at 5% and 10%. The internal transmittance of a 1-meter externally heated absorption cell was measured. The results establish a value for the absorptivity, α, for CO_2 ranging as high as 2.35×10^{-19} cm^2/molecule at 1600 °C. For O_2 the absorptivity is 1.81×10^{-19} cm^2/molecule at 1600 °C. The results partially agree with those reported in the literature recently by others at 1000 °C and 193 nm and extend those data to higher temperatures, however, the agreement is far from exact. The results are inconsistent with the higher temperature, 1500–2500 °C, values inferred by others from indirect measurements for these two species.

Introduction

Many laser-based diagnostics of combustion systems are in use today, employing the entire optical spectrum from the ultraviolet to the infrared. The goal of most of these techniques is to obtain quantitative measurements of specific chemical species at temperature conditions typically ranging from 1000 °C to 1700 °C. Key applications include engine and combustor optimization diagnostics and thermal waste treatment monitoring. Many potentially sensitive techniques are based on 193 nm ArF laser excitation, but are limited by difficulties associated with either excitation or detection efficiencies near this wavelength at high temperature. A major source of these problems is the temperature dependent absorptivity of high concentrations molecular oxygen and carbon dioxide, which are always present to some degree in a combustion environment. For example, these species are major constituents of the gas phase in glass melting furnaces, for which Excimer Laser Induced Fragmentation Fluorescence (ELIF) is under consideration as an in-situ method to detect NaOH(gas) (see Chap. 5).

Recently, Joutsenoja et al.[1] have reported detailed measurements of the absorptivity of these two species up to 1700 K and at wavelengths as short as 200 nm. Hildenbrand et al.[2] present CO_2 absorptivities as a function of temperature and wavelength to 2300K and 200 nm based on the work of Jensen et al.[3] The experiments in Ref. 2 highlight the need for this type of quantitative information. The trend in these 200 nm data indicates that the absorptivities are likely to be even greater at 193 nm, as would be expected.

One potential spectroscopic method for detecting trace species in a combustion environment that has received considerable attention recently is Excimer Laser Induced Fragmentation Fluorescence (ELIF) or Laser Induced Atomization (LIA). It has been shown that this technique can be very sensitive for detecting metals in high temperature vapor environments[4,5] and, in particular, a number of authors have explored the use of this method to determine alkali concentrations in solid fuel combustors.[6-10] The general ELIF technical approach is to illuminate the vapor containing simple molecular metal-containing species, such as NaOH, NaCl, KOH, etc., with a 193 nm laser pulse from an ArF laser. The subsequent photodissociation produces a population of excited metal atoms which produce atomic emission lines that are easy to detect.

In our work, the need to better understand the absorptivity of these gases stems from the application of ELIF as a means to examine the details of gas composition in glass manufacturing furnaces. In this instance, the vapor temperature can range from 1000 °C to as high as 1700 °C and recent work[11] has shown the important role trace alkali vapor can play in the rate of degradation of the refractory material from which these furnaces are constructed. ELIF represents a potential diagnostic method to access the spatial and temporal concentration dynamics of key alkali species.

The groups exploring ELIF as a combustor diagnostic have identified a number of practical considerations that must be addressed to obtain quantitative species concentrations from the atomic fragment fluorescence, include fluorescence quenching,[12] radiation trapping,[13] and probe beam absorption.[14] This last issue, the depth of excimer laser penetration into the hot gases, becomes more important at the higher temperatures experienced in a glass furnace. Clearly, the development of this photodissociation effect into an analytical technique for in situ measurements in furnaces and combustors relies on the ability to determine the intensity of the probe beam at a particular point in the combustion environment. The work of Hartinger et al.[14] provides the most recent and thorough examination of the absorption of 193 nm light by O_2 and CO_2, but only up to 1000 °C. However, they report that both species exhibit marked temperature dependence in their absorptivity at this wavelength. The absorptivity of oxygen at ambient and elevated temperature at this wavelength has been well studied,[15-20] but other than these data in Ref. 14, no other direct measurements have been reported on CO_2 at 193 nm.

Koshi et al.[21] report effective absorptivity values for O_2 and CO_2 at 193 nm in very dilute mixtures measured indirectly behind shock waves fin a temperature range of 1200–2400 °C. They report that $\alpha = 9 \times 10^{-20}$ cm^2/molecule for O_2 at 1500 °C and $\alpha = 4 \times 10^{-20}$ cm^2/molecule for CO_2 at 1500 °C. These CO_2 data are the only available in this temperature range and 193 nm prior the results we report here. They report that the $\alpha(O_2)$ is less than that reported by Davidson et al.[18] who place $\alpha(O_2)$ at 2.0×10^{-19} cm^2/molecule at 1500 °C. An extrapolation of the values that Hartinger et al.[14] report at 1000 °C to higher temperature is not consistent with the data on either species in Ref. 21, being higher at a given temperature, but lower than the results for O_2 in Ref. 18. The results reported by Joutsenoja in Ref.1, when extrapolated to 193 nm from 200 nm generally appear to agree with Ref 14, given the uncertainty in such an extrapolation. This paper reports the absorptivity of CO_2 and O_2 up to 1600 °C. Primarily, the results are intended to address the discrepancy between the 400–1000 °C data from Refs. 14, as well as the data in References 1 and 18 with the high temperature shock tube data of Ref. 21.

Experimental Method

Transmittance measurements of CO_2 and O_2 were conducted in a high temperature tube furnace designed to have a slow flow of a variety of gas mixtures. The apparatus is illustrated in Figure A-1. A 1600 °C (maximum) tube furnace (Carbolite STF) equipped with a 5 cm diameter alumina sample tube and capped with synthetic fused silica windows in Teflon holders, functions as the spectroscopic cell. The windows are 0.63 cm (0.25 in nominal) thick. The total cell length is 103 cm. The furnace consists of six SiC heaters that radiatively heat the sample tube. Each end of the tube is outside the heated region and there is a 10 cm length of alumina insulation within the furnace that is exposed to the radiative heaters, but prevents direct radiative transfer from the SiC rods to the sample tube. Gases are mixed at ambient temperature and are injected into the tube at one end and leave the tube at the other end, drawn out by the draft ventilation. The total flow rate in the tube is typically 3000 std cc/min yielding a flow pattern that is laminar with over the temperature range explored here. However, the large thermal gradients at the inlet and outlet of the furnace will disturb these flow conditions, enhancing the radial mixing of the gas. The average flow velocity ranges from 2.5 cm/s at the relatively cool injector to 15 cm/s in the center of the furnace. The laminar flow centerline velocity is as high a 30 cm/s.

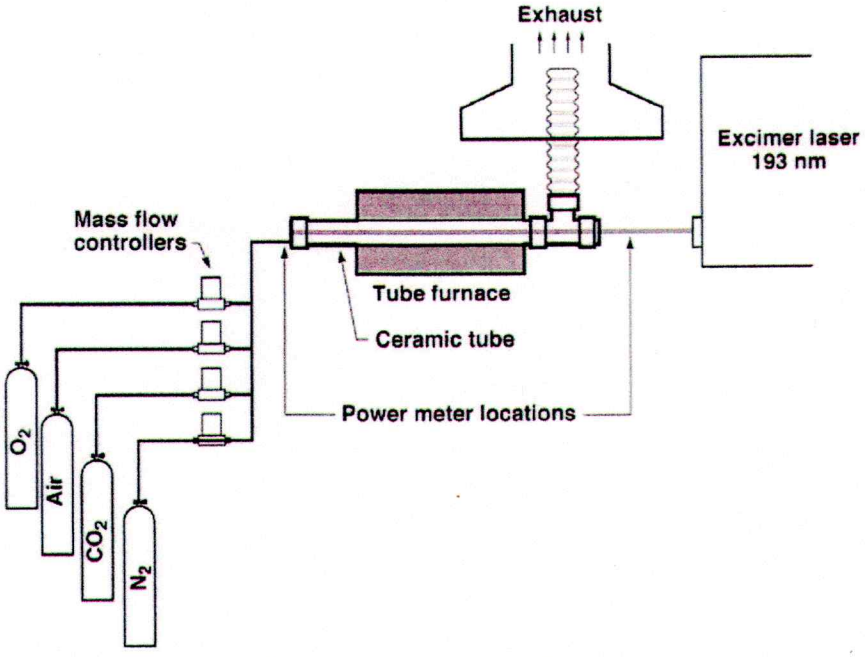

Figure A-1. Schematic of the high-temperature flow cell apparatus used to measure the absorptivity of O_2 and CO_2 or T≤ 1600 °C.

Axial temperature profiles at experimental conditions within the furnace were measured using an exposed 0.38 mm (0.015 in) Type "B" thermocouple that could be moved to any point along the centerline of the tube by way of an adaptor on the gas inlet end of the tube. The wire leads were confined within separate holes running the length of a two-holed alumina rod. The bare thermocouple junction was exposed with a length of wire of approximately 0.4 cm. Temperatures were measured on the tube wall and on the centerline. Temperatures were also measured on the centerline using a 0.075 mm (0.003 in) bead Type R thermocouple.

The measured centerline gas temperatures were corrected for radiation effects using the method outlined by Shaddix.[22] In this calculation, the emissivity of the Pt- Pt/Rh thermocouples ranged from 0.15 at 1000 °C and below to 0.19 at 1500 °C, following Ref. 1. In general, corrections were less than 100 °C for the large thermocouple and less than 20 °C for the small one. The corrected values for the two measurements are in good agreement, producing values for the true gas temperature within 20 °C of each other.

Figure A-2 shows a subset of the series of curves that relate the temperature profiles within the furnace to the nominal furnace temperature set point. The figure shows the measured temperature at the wall and the corrected temperature on the centerline of the tube. The wall temperature at a given position is used as the temperature of the radiative environment for the corrections to the measured gas temperatures. Axial profiles were recorded every 100 °C from 900 °C to 1600 °C. The temperature was measured at 2 cm intervals along the entire length of the tube with the probe being inserted from the downstream end to minimize disturbance on the flow due to the probe.

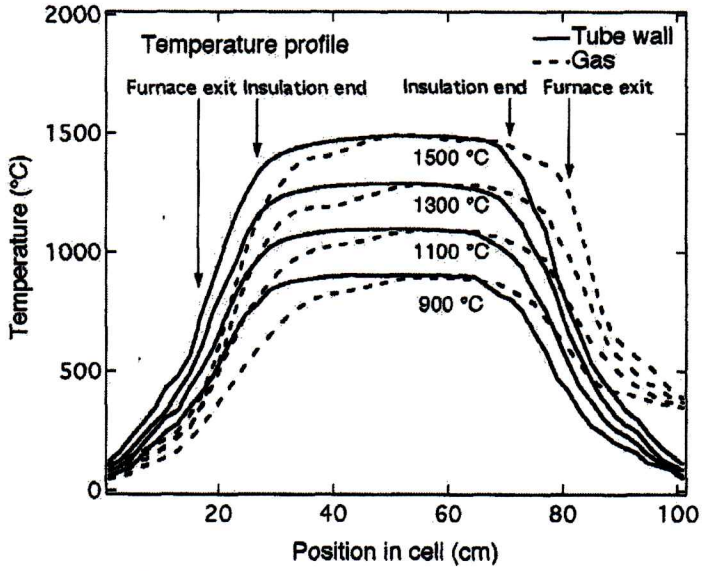

Figure A-2. Temperature profiles within the tube furnace of the tube wall (solid line) measured directly by a thermocouple and the gas temperature (dashed line) at the center of the tube corrected for radiation effects.

The internal transmittance measurements consist of several sets of data recorded in identical fashion. A 193 nm ArF laser (GAM Laser model EX10), operating at a nominal pulse energy of 12 mJ/pulse at 100 Hz and 0.5-nm line width, served as the source of the UV light. The beam was not focused and has an approximate cross section 3 x 8 mm. The average input power was measured using a factory-calibrated pulsed-laser power meter (Coherent Fieldmaster GS) placed 4 cm in front of the input window. To measure transmittance, the same meter was moved to a position 1 cm outside of the exit window. The gas mixtures examined were pure N_2, 5% CO_2 in N_2, and 5% and 10% O_2 in N_2. The fractional composition of the gas was determined by volumetric flow rate in the gas manifold measured by mass flow meters (Brooks Model 5850).

As both O_2 and CO_2 are known to dissociate upon excitation at 193 nm, some of the transmittance measurements were repeated with a laser pulse energy of 6 mJ/pulse and the laser pulse repetition rate was varied from 20 to 300 Hz. Changes in the internal transmittance are small relative to the overall experimental accuracy and do not appear to be systematic. If photolysis products contribute to the overall absorptivity at these conditions, a significant variation in the measurements as a function of these two parameters would be expected.

Results and Discussion

Figure A-3a presents a plot of the transmitted intensity of a 0.05 volume fraction mixture of CO_2 in N_2 as well as a curve representing the pure N_2 reference as a function of nominal setpoint temperature, Θ, in the flow furnace. Figure A-3b shows similar data for O_2 at both 0.05 and 0.10 volume fraction. The incident intensity of the 193-nm light is attenuated by the 4 cm of air in front of the window and reflection losses at the input and exit windows. We have measured these properties of our system directly. The attenuation by ambient air is <1%, the reflection losses at the uncoated fused silica window is 4.7% at each surface, and the absorption is about 6%, but appears to be temperature dependent. Thus, the transmittance of the apparatus at ambient temperature is 62.8% when filled with nitrogen and is represented by the data at ambient temperature in nitrogen in Figure A-3. As the input and exit windows can reach temperatures as high as 200 °C, the reduction in transmission of the reference N_2 sample, shown if Figure A-3, originates from the temperature dependence of the window reflection and absorption characteristics. For the analysis described below, the input and exit intensities are corrected for these losses.

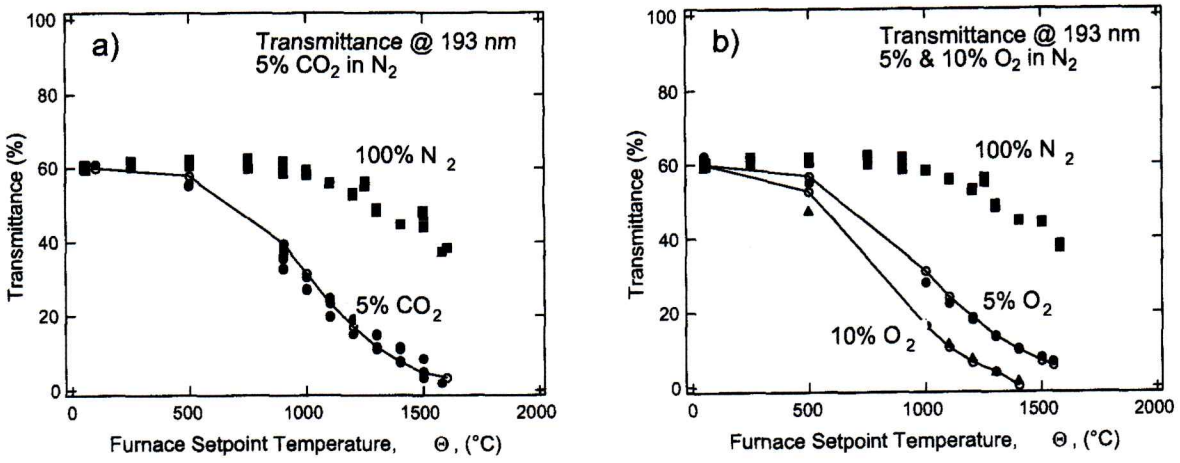

Figure A-3. a) Measured and fitted results for CO_2 transmittance in the high temperature cell vs. b) furnace setpoint temperature, Θ. Pure N_2: solid squares, 5% CO_2 in N_2: solid circles, results from fitted parameters from Table A-1: open circles/line. b) Measured and fitted results for O_2 transmittance in the high temperature cell vs. furnace setpoint temperature, Θ. Pure N_2: solid squares, 5% O_2 in N_2:solid circles, 10% O_2 in N_2:solid triangles; results from fitted parameters from Table A-1: open circles/line.

The data in Figure A-3 represent the transmission of the 193-nm light through the temperature profiles shown in Figure A-2 with temperatures on the abscissa being the nominal setpoint values of the furnace. Scatter in the data originates mostly from the precision of the mass flow meters. The error in these raw data carries over to the standard deviations reported for the fitted absorptivity parameters.

The raw transmission data are the result of the combination of the gas mixture absorptivity, which varies with temperature across the temperature profile, and the density profile within the furnace. Hartinger et al.[14] have suggested that the absorptivity for both O_2 and CO_2 follow an exponential functional form in temperature, at least up to 1000 °C. This is not surprising as the 193-nm absorption originates from thermal population of excited vibrational levels. Thus, for each molecule, if a parameterized exponential functional form for the absorptivity is assumed, the transmittance data in Figure A-3 can be fitted to the direct numerical integration of

$$dI_t(z) = - I_t(z)\alpha(T_\Theta(z))\rho(T_\Theta(z))dz \qquad \text{(A-1)}$$

where $I_t(z=0)$ is the input intensity after correction for the input losses at the window, $T_\Theta(z)$ is represented by the gas temperature curves in Figure A-2 for a given furnace setpoint temperature Θ, z is the axial position within the tube/cell, and α is the molecular absorptivity. The measured transmittance is $I_t(z = 103$ cm) corrected for the exit window losses. The function, $\rho(T_\Theta(z))$ is taken as the density of an ideal gas, $P/R\ T_\Theta(z)$. The molecular absorptivity at a given point in the furnace is represented by

$$\alpha(T_\Theta(z)) = \alpha_o \exp(-\varepsilon/T_\Theta(z)) \qquad \text{(A-2)}$$

where ε, and α_o are fitting parameters, having no physical meaning themselves. The parameters, ε and α_o, are determined for both CO_2 and O_2 by a non-linear least squares fitting process to the transmittance measurements for each species recorded at the different values of Θ. The data is fitted to minimize the variance of the logarithm of the measured transmittance. This functional form best provides equal weighting of the individual temperature points in determining α_o and ε. The results to the fits are listed in Table A-1. Figure A-3a and A-3b show the results of the fits by plotting the calculated absorptivity curves from the fitted parameters along with the raw transmittance data.

Table A-1. Fitted parameters for absorptivity, $\alpha(T) = \alpha_o \exp(-\varepsilon/T)$ (cm^2/mol)

	ε(K)	$\sigma(\varepsilon)^a$	α_o (cm^2/molecule)	$\sigma(\alpha_o)^a$
CO_2	6327	429	6.89×10^{-18}	1.92×10^{-18}
O_2	5475	270	3.37×10^{-18}	0.63×10^{-18}

(a) – 1σ error from fit

It is well known that O_2 absorbs appreciably at 193 nm, even at ambient temperatures, and has an absorption coefficient that exhibits a direct dependence on the product of pressure and pathlength, *Pz*, such that the Beer-Lambert Law is not followed. Lee and Hanson[17] illustrate that the effect of elevated temperature is insufficient to smooth out the spectral structure within the 0.5 nm ArF laser bandwidth and thus, the absorptivity is not independent of the product of the pressure and pathlength over the range of temperature examined here. This is due to the complicated nature of the spectrum consisting of overlapping features of discrete predissociated transitions with individual linewidths much sharper than the laser line. In contrast to O_2, the absorption spectrum of CO_2 is diffuse and therefore the absorptivity is independent of *Pz*.[14] However, for the 5% measurements, the value of *Pz* is small. With the partial pressure of O_2 only 0.05 bar, and the effective high-temperature region, which contributes to the bulk of the absorption, only about 40 cm (see Figure A-2), the resulting *Pz* is near 2 bar-cm. Examination of the *Pz* dependence in Ref. 14 shows that the precision of data reported here cannot distinguish between a value of 2 and a value of zero for *Pz*. According to the results in Ref. 14, we would expect to see an effect on the absorptivity at the 0.10 bar partial pressure. Here, however, the same absorptivity values reproduce the data in the measurement at both concentrations.

The functions $\alpha(T)$ for CO_2 and O_2 are plotted in Figures A-4 and A-5 respectively. The results are compared with those reported by Hartinger et al.[14] in the relatively simple case of CO_2 using Eq. A-5 in that paper for k and converting to α through the relationship $\alpha = k$RT and $R = 1.38 \times 10^{-22}$ bar-cm^3/molec-K. In the case of O_2, we have used their $Pz = 0$ equation (Eq. A-6) for comparison, similarly.

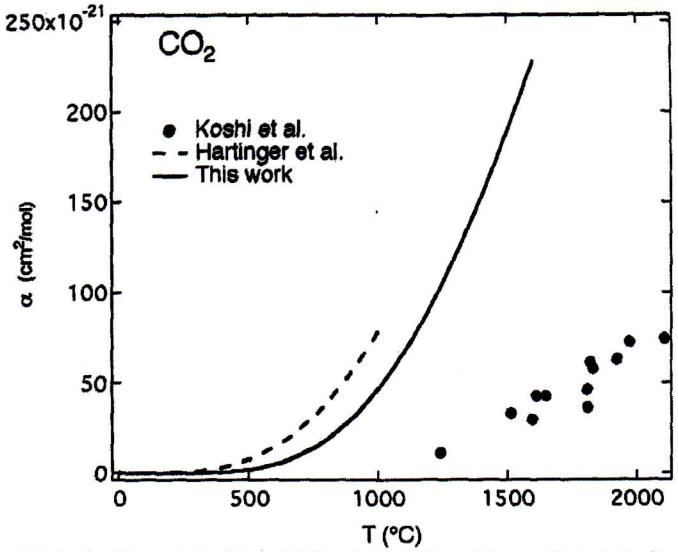

Figure A-4. Absorptivity of CO_2 determined from the data in Figure A-3 using the method described in the text and the parameters in Table A-1 (solid line). Included in the figure are the results reported by Hartinger et al.[14] (dashed line) and data take from Koshi et al.[21] (solid circles).

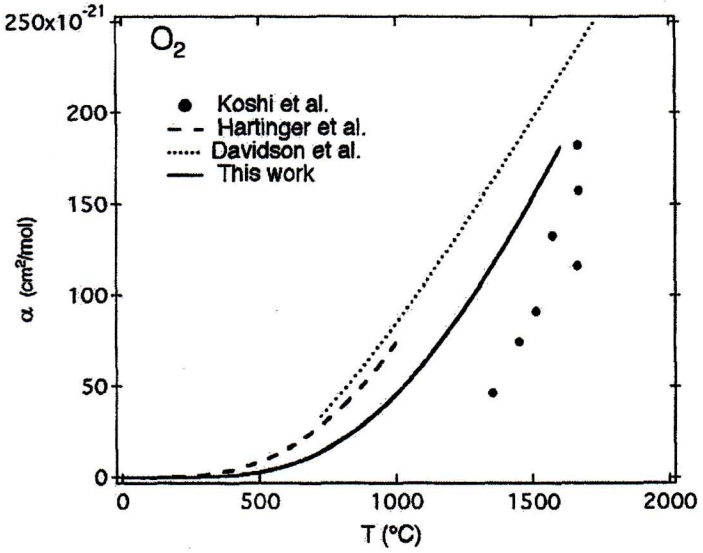

Figure A-5. Absorptivity for O_2 determined from the raw transmittance data using the method described in the text. Included in the figure are the results reported by Hartinger et al.[14] (dashed line) and data take from Koshi et al.[21] (solid circles). The dotted line is the function Davidson et al for k in atm^{-1}-cm^{-1} converted to α in cm^2/molecule.

The results presented in Figures A-4 and A-5 place the absorptivity of both O_2 and CO_2 at a value somewhat less that that reported by Hartinger et al.[14] at for the region of overlap. Extrapolation of the Ref. 14 CO_2 curve to higher temperature produces an offset between these two measurements of about 45 x 10^{-21} cm^2/molecule. The results in Ref. 1, extrapolated to 193 nm, yield approximately 250 x 10^{-21} at 1400 °C, which is greater than the formula in Ref. 14 would predict by nearly a factor of two. Thus, there remains some discrepancy among the various studies.

The situation for O_2 is similar. Again, the results presented here indicate an absorptivity that is somewhat lower than that observed and extrapolated in Ref. 14, which agrees well with Ref. 18. An extrapolation of the results in Ref. 1 to lower wavelength will produce an absorptivity that is nearly twice that reported in Ref. 14. The disagreement between these new results presented here and those in Ref. 1 is even greater.

Conclusion

Parameters for exponential-type functions that represent the absorptivity of CO_2 and O_2 at 193 nm from an ArF laser over the temperature range of 900-1600 °C are determined from transmittance measurements in a high temperature cell. The results indicate that the combined set of measurements on O_2 and CO_2 at 193 nm using this work and the data in Ref. 14 and Ref. 1 provide an evaluation of the absorptivity of these molecules at high temperature conditions, but the agreement among the data sets is not ideal. The new data indicate that the earlier reported values in Ref. 21 are too low, especially for CO_2. These new results contribute to the quantitative spectrometric knowledge of these two key combustion gases for the development of excimer laser-based probes of furnace environments.

References

[1] T. Joutsenoja, A. D'Anna, A. D'Alession and M.I. Nazzaro, Appl. Spectrosc. **55**, 130 (2001).

[2] F. Hildenbrand, C. Schultz, Appl. Phys. B **73**, 173 (2001).

[3] J.R. Jensen, R.D. Guettler, J.L Lyman, Chem. Phys. Lett. **277**, 356 (1997).

[4] S.G. Buckley, C.P. Koshland, R.F. Sawyer, D. Lucas, Proc. Comb. Inst. **26**, 2455 (1996).

[5] S.G. Buckley, C.S. McEnally, R.F. Sawyer, C.P. Koshland, D. Lucas, Combust. Sci. Technol. **118**, 168 (1996).

[6] K.J. Rensberger Welland, M.L. Wise, and G.P. Smith, Appl. Opt. **32**,4066 (1993).

[7] K.T. Hartinger, P.B. Monkhouse, J. Wolfrum, H. Baumann, and B. Bonn, Proc. Comb. Inst. **25**, 193 (1994).

[8] B.L. Chadwick, G. Domazetis, R. J.S. Morrison, Anal. Chem. **67**, 710 (1995)

[9] F. Greger, K.T. Hartinger, P.B. Monkhouse, J. Wolfrum, H. Baumann, and B. Bonn, Proc. Comb. Inst. **26**, 3301, (1996).

[10] P.G. Griffin, R.J.S. Morrison, A. Campisi, B.L. Chadwick, Rev. Sci. Instrum. **69**, 3674 (1998).

[11] M.D. Allendorf, K.E.Spear, J. Electrochem. Soc. **148**, B59 (2001).

[12] K.T. Hartinger, S. Nord, and P.B. Monkhouse, Appl. Phys. B, **64**, 363 (1997).

[13] B.L. Chadwick and R.J.S. Morrison, J. Chem Soc. Faraday Trans. **91**,1931 (1995).

[14] K.T. Hartinger, S. Nord, and P.B. Monkhouse, Appl. Phys. B **70**, 133 (2000).

[15] M. Ogawa, J. Chem. Phys. **54**, 2550 (1971).

[16] M.W.P. Cann, J.B. Shin, and R.W. Nichols, Can. J. Phys. **62**, 1738 (1984).

[17] M.P. Lee and R.K. Hanson, J.Quan. Spectrosc. Radiat. Transfer **36**, 425 (1986).

[18] D.F. Davidson, A.Y. Chang, K. Kohse-Höinghaus, and R.K. Hanson, J.Quan. Spectrosc. Radiat. Transfer **42**, 267 (1989).

[19] M. Shimauchi, T, Miura, and H. Takuma, Jpn. J. Appl. Phys. **33**,4628 (1994).

[20] J. Vattulainen, L. Wallenius, J. Stenberg, R. Hernberg, and V. Linna, Appl. Spectrosc. **15**, 1311 (1997).

[21] M. Koshi, M. Yoshimura, and H, Matsui, Chem. Phys. Lett. **176**, 519 (1991).

[22] C. R. Shaddix, Proceedings of the 33rd National Heat Transfer Conference FTD99-282 August 15-17, Albuquerque, NM (1999).